

PAPER

Deep-Reinforcement-Learning-Based Distributed Vehicle Position Controls for Coverage Expansion in mmWave V2X

Akihito TAYA[†], *Student Member*, Takayuki NISHIO^{†a)}, *Member*,
Masahiro MORIKURA[†], *Fellow*, and Koji YAMAMOTO[†], *Senior Member*

SUMMARY In millimeter wave (mmWave) vehicular communications, multi-hop relay disconnection by line-of-sight (LOS) blockage is a critical problem, particularly in the early diffusion phase of mmWave-available vehicles, where not all vehicles have mmWave communication devices. This paper proposes a distributed position control method to establish long relay paths through road side units (RSUs). This is realized by a scheme via which autonomous vehicles change their relative positions to communicate with each other via LOS paths. Even though vehicles with the proposed method do not use all the information of the environment and do not cooperate with each other, they can decide their action (e.g., lane change and overtaking) and form long relays only using information of their surroundings (e.g., surrounding vehicle positions). The decision-making problem is formulated as a Markov decision process such that autonomous vehicles can learn a practical movement strategy for making long relays by a reinforcement learning (RL) algorithm. This paper designs a learning algorithm based on a sophisticated deep reinforcement learning algorithm, asynchronous advantage actor-critic (A3C), which enables vehicles to learn a complex movement strategy quickly through its deep-neural-network architecture and multi-agent-learning mechanism. Once the strategy is well trained, vehicles can move independently to establish long relays and connect to the RSUs via the relays. Simulation results confirm that the proposed method can increase the relay length and coverage even if the traffic conditions and penetration ratio of mmWave communication devices in the learning and operation phases are different.

key words: Vehicular networks, Autonomous vehicles, mmWave communications, Multi-hop relaying, Position controls, Deep reinforcement learning

1. Introduction

Autonomous and connected vehicles can not only achieve safe and efficient transportation but can also provide several intelligent services such as real-time detailed maps, vehicular cloud computing, cooperative perception, and infotainment [1–4]. Some of these services require high-throughput vehicle-to-infrastructure (V2I) communication, which is one of the reasons why millimeter-wave (mmWave) vehicular communications have attracted considerable attention [3, 5–7].

Although mmWave communications can achieve high-throughput data transmission, their communication ranges tend to be shorter than microwave communications because of their high attenuation. This makes the communication coverage of road side units (RSUs) smaller. For microwave vehicular communications, multi-hop relaying has been

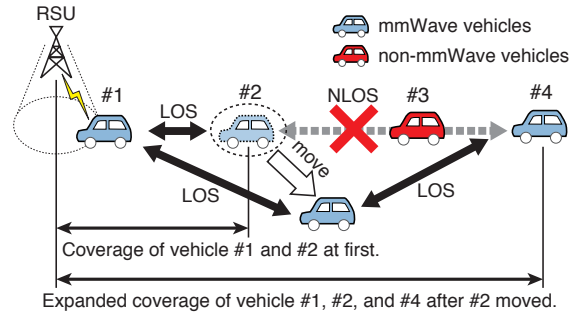


Fig. 1 Vehicle #3 initially blocks the path between vehicles #2 and #4. When vehicle #2 changes its position, vehicles #2 and #4 communicate with each other via a LOS path; thus, the multi-hop relay becomes long.

studied to extend the coverage of RSUs [8–10]. Multi-hop relaying is significantly more important for mmWave communications because of their short communication range. However, mmWave relaying presents a major challenge in the form of its disconnection problem. In mmWave vehicle-to-vehicle (V2V) relaying, the line-of-sight (LOS) path is easily blocked by other vehicles, particularly vehicles that do not have the capability of mmWave relaying. Therefore, mmWave V2V relay networks can be disconnected and fragmented frequently because mmWave signals are severely attenuated by the blockages. This disconnection induced by the blockage is critical, particularly in the diffusion phase of mmWave-available vehicles, where not all vehicles have mmWave communication devices.

This paper studies a vehicle position control method to solve the relay disconnection problem and extend the coverage of RSUs. The proposed method enables position-controllable vehicles, such as autonomous vehicles, to change their relative positions, where LOS paths are available and V2V relays can be connected by lane change or overtaking. Figure 1 shows a simple example of our method. Let vehicles #1, #2, and #4 have mmWave communication devices, while vehicle #3 does not have one. Vehicles #1 and #2 are initially connected with each other on mmWave channels, but vehicles #2 and #4 are not connected because of the blockage by vehicle #3. In this case, by moving vehicle #2 to a position where a LOS path between vehicle #2

Manuscript received January 1, 20xx.

Manuscript revised January 1, 20xx.

[†]The author is with the Graduate School of Informatics, Kyoto University, Yoshida-honmachi, Sakyo-ku, Kyoto, 606–8501 Japan.

a) E-mail: nishio@i.kyoto-u.ac.jp

DOI: 10.1587/transcom.E0.B.1

and #4 becomes available, the relay length can be extended and thus, the RSU coverage is extended to include vehicle #4.

Cooperative position controls of vehicles have been studied in [11–14]. While they focus on improving the stability and robustness of formation and platooning control, they do not consider improving communication quality. In the fields of robots and wireless sensors, movement or position control methods to improve the connectivity of multi-hop communications have been discussed [15, 16]. However, these prior works do not focus on the relay length, and they consider conventional microwave communications where no harmful blockage occurs.

Our previous work proposed a vehicle position control method for coverage expansion in mmWave vehicular networks and revealed the maximum gain of coverage improvement by optimizing vehicle positions [17]. However, this work uses a centralized algorithm, which is not sufficiently scalable, and does not consider the movement of each vehicle to its optimal position. To maximize the relay length, both positions of vehicles and their movement paths should be optimized. However, the optimization problem of collision-free path planning of multiple vehicles is an NP-hard problem [18]. Therefore, the optimal solution cannot be obtained even if centralized manners are applied. Moreover, centralized algorithm is not practical for vehicle controls because it cannot be applied when lots of vehicles exist in wide area, thus a distributed mechanism is required that enables vehicles to expand relay length by moving to good positions without collision.

In this paper, we develop a deep-reinforcement-learning (DeepRL)-based vehicle position control method, where each vehicle distributedly decides its movement without knowledge of the optimal position or global information other than that of the surrounding vehicles. Reinforcement learning (RL) is introduced to obtain a movement strategy via which vehicles decide their movement in order to increase coverage based on their own information, such as locations of the surrounding vehicles. Because such a strategy is high-dimensional and non-linear function, we employ DeepRL, which combines RL algorithms and deep learning methods. To increase the learning speed by updating the strategy cooperatively, we leverage a distributed DeepRL algorithm, asynchronous advantage actor-critic (A3C) [19], which was originally developed for parallel processing. In A3C, multiple agents update the shared strategy cooperatively, while acting in multiple environments independently. By applying the cooperative-strategy-updating scheme to our coverage-improvement problem, multiple vehicles can cooperatively and efficiently learn the strategies; this allows them to make decisions without communicating with each other. Because DeepRL algorithms achieve high performance in problems where the environment state is represented as a pictorial image, we design a three-dimensional state representation like color images for the coverage expansion problem.

Our simulation results show that vehicles can learn the coverage-increasing strategy using the DeepRL algorithm.

We also demonstrate that the learned strategies achieve high performance even when the traffic conditions and the penetration ratio of mmWave-available vehicles are changed from that in the learning phases.

The contributions of this paper are summarized as follows:

- (1) We present a solution for blockage problems in mmWave vehicular networks. The proposed method is based on position control of vehicles, whereas conventional works [8–10] have assumed that vehicle positions are specified and not controllable.
- (2) We present a distributed DeepRL-based vehicle movement-control algorithm. By leveraging a DeepRL algorithm, A3C, our algorithm enables vehicles to learn a movement strategy, which involves complex mapping from surrounding vehicle positions to movement action.
- (3) The simulation results justify that the proposed algorithm achieves high performance even when the environment conditions (e.g., the penetration ratio of mmWave-communicable vehicles and vehicle density) of learning and test phases are not the same.

The rest of this paper is organized as follows: Related works are discussed in Section 2. Then, our system model is described in Section 3, and the DeepRL-based approach to improve coverage is presented in Section 4. Finally, simulation results are presented in Section 5 and the conclusions are drawn in Section 6.

2. Related Works

2.1 Vehicular Networks

One of the current available vehicular communication protocols is dedicated short range communication (DSRC). DSRC, which has been standardized as IEEE 802.11p, uses the 5.8–5.9 GHz band [20]. Another protocol is cellular vehicle-to-everything (C-V2X), which is specified in the third generation partnership project (3GPP) Release 14 [21]. Unfortunately, these protocols cannot meet the increasing demand of high-data-rate vehicular communications for sharing enormous sensor data and providing infotainment because of their limited bandwidth.

Therefore, mmWave communication is an essential technique for vehicular communications to meet the increasing demand. MmWave communications offer huge bandwidth (e.g., 9 GHz in 60 GHz band) and realize beyond-Gbit/s throughput. In addition, offloading data transmission of non-safety applications from the microwave bands to the mmWave bands can reduce the pressure on the microwave band, and should be used for critical applications such as vehicle collision warning systems and self-driving systems. The authors of [3] provide a survey of mmWave vehicular communications, including detailed analysis of mmWave spectrum, PHY, and MAC designs for mmWave communications that can be applied to vehicular communications. MAC

protocols for mmWave multi-hop relaying for vehicular networks have been studied in [7, 22]. In [22], an ALOHA-based protocol is evaluated for a one-lane highway scenario, and it is demonstrated that multi-hop achieves better performance than single-hop in disseminating information to a certain number of vehicles. The authors of [7] study content delivery using heterogeneous networks consisting of the licensed Sub-6 GHz band, DSRC, and mmWave communications. They introduce fuzzy logic to select efficient cluster heads considering the vehicle velocity, vehicle distribution, and antenna height. Whereas these studies assume that vehicle movements are given, we propose to control vehicle movements in order to avoid blockage.

Multi-hop relaying for increasing the coverages of RSUs has been studied for the microwave vehicular adhoc network (VANET). The authors of [8] propose multi-hop V2V relaying to compensate for the sparsity of RSUs. [9] minimizes the number of vehicles that communicate with RSUs by constructing clusters where messages are transmitted via V2V relays. The authors of [10] propose a forwarding algorithm to extend the coverage of RSUs for urban areas. The algorithm realizes multi-directional dissemination in intersections by considering the geographic positions of vehicles. Although these prior studies show high performance when the vehicle density is high, relay disconnections by obstacles are not considered because these studies assume microwave VANETs. We leverage the mobility controllability of autonomous vehicles to connect vehicles via LOS paths. Such a topology-modifying scheme is one of the differences between our method and conventional methods.

Position control of vehicles has been studied in the literature of cooperative vehicle platoon and formation controls [11–14]. The authors of [11] develop a platoon-management protocol based on VANET. In the protocol, the platoon leader sends beacons that contain platoon parameters to followers in a multi-hop manner, and each follower maintains an appropriate inter-vehicle space. [12] proposes an intra-platoon management strategy that ensures platoon stability under the presence of communication delays. The authors of [13, 14] study formation controls for cooperative vehicles. They utilize graph theory and demonstrate the robustness of their methods. In [23], a formation-control method based on potential fields is proposed for unmanned aerial vehicles. Although these methods, which rely on vehicular communication techniques, improve the stability or robustness of vehicle formations, they are not intended to improve communication quality. Moreover, they assume that the desired patterns or inter-vehicle distances are given, whereas our work focuses on finding the relative positions that increase the coverage of wireless networks. To our knowledge, such approaches that control vehicle positions on the road in order to improve communication quality have not been studied.

Some researchers of robot control systems, not vehicles, have proposed movement control or positioning schemes to improve the connectivity of multi-hop networks. The authors of [15] propose a block-movement algorithm to construct fault-tolerant adhoc networks for autonomous multi-

robot systems. However, coverage expansion is not discussed in [15]. As a decentralized deployment method, virtual force algorithms (VFAs) are introduced in [24, 25]. These algorithms focus on increasing the sensor coverage of wireless sensor networks (WSNs) under the constraints of the desired connectivity. VFAs are also used in [16] for vehicle self-deployment in order to form fault-tolerant adhoc networks. The authors of [16] utilize an evolutionary algorithm (EA) to determine the velocity and virtual forces for fitness values of the EA. VFAs perform well in these studies because they assume microwave communications, in which connection quality between two nodes increases as they become closer. In mmWave communications, however, blockage effects decrease the connectivity of non-line-of-sight (NLOS) communications; thus, mmWave connectivity, as a function of positions, has local maxima. Therefore, VFAs, which are based on gradients, are not expected to improve mmWave connectivity because vehicles are trapped at the local maxima.

Note that other approaches to solve the blockage problem are discussed, and beamforming is a promising technique that controls the directionality of array antennas to leverage a strong reflected signal [26–28]. Our work does not conflict with beamforming and can be used simultaneously. For example, when a LOS path is not available but a NLOS path with a strong signal is available, beamforming solves the blockage problem. However, if there are no LOS and strong NLOS paths, our method moves vehicles to leverage a strong path and extend the relay length.

2.2 Reinforcement Learning

Reinforcement learning has been developed to solve the problem of a mapping from situations to actions so as to maximize a reward in an environment [29, 30]. In RL, an agent learns the mapping by performing actions and observing the results of the actions in the environment. Although table-based Q-learning, which is one of the most widely used RL algorithms, is guaranteed to solve the simple Markov decision process (MDP), it cannot be applied to large-scale problems due to a limitation of computational memory capacity. Because of recent studies, RL using deep neural networks (DNN) for function approximation can solve large-scale problems such as video games [31] and the ancient board game Go [32]. Moreover, multi-process learning algorithms, such as general reinforcement learning architecture (Gorila) [33] and A3C [19], have been developed to improve the convergence efficiency and learning speed. In A3C, multiple agents learn their strategies in independent environments and asynchronously share the strategies. We utilize A3C to solve our coverage-improvement problems in order to improve learning speed by cooperative learning.

3. System Model

Figure 2 illustrates our system model. We consider a straight N_1 -lane highway with mmWave RSUs deployed at intervals

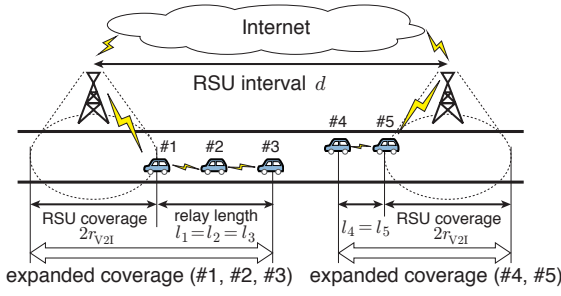


Fig. 2 Coverage is expanded through multi-hop relaying. l_i denotes the length along the x axis of the relay chains to which vehicle i belongs. The expanded mmWave V2I communication range of vehicle i can be expressed as $2r_{V2I} + l_i$.

of d . We only consider a single direction as our aim is to create relay chains that remain unchanged for a long time. For simplicity, we assume that vehicles are located at grid points. We assume that the average velocities of all the vehicles are nearly the same, which is confirmed in [34], where the authors demonstrate that velocity variance decreases as the ratio of vehicles with adaptive cruise control increases, which is one of the key technologies in autonomous vehicles. We also consider two cases in the simulation evaluations: one where the velocity is constant and the other where it fluctuates. When the vehicles move at a constant and equal velocity, the relative positions of the vehicles do not change. When the velocity fluctuates, the movements on the relative positions can be modeled as random walks. A region of interest (RoI) also moves with the vehicles at the same velocity as them.

A simplified mmWave communication model is assumed in which vehicles can be connected if and only if the distance between the vehicles is less than a certain distance and a LOS path is available. We also assume that link qualities of the mmWave channels are ideally predictable. This assumption is not unrealistic considering state-of-the-art prediction methods. For example, the authors of [6, 35] present a mmWave propagation loss model for V2V communications. Another approach is proposed in [36, 37], where the authors predict the throughput of mmWave communications and received signal strength of mmWave radios using image sensor data.

There are non-mmWave vehicles and mmWave vehicles, which are subdivided into controllable mmWave vehicles and uncontrollable mmWave vehicles. Whereas the non-mmWave vehicles only use microwave communication systems, mmWave vehicles use both microwave and mmWave communication systems and constitute the multi-hop relay chains for increasing coverage. Microwave communication systems, such as DSRC and C-V2X, enable all the vehicles to share information on vehicle positions and their control signals, whose packet sizes are very small. We assume that the

effect of transmission loss and delay is negligible because the duration for a transmission is less than 100 ms which is much less than the decision-making interval of vehicles. For example, in DSRC, the vehicles broadcast their position every 100 ms [20]. Therefore, the vehicles can retransmit dropped packets several times and the probability that the vehicles fail to receive all the retransmitted packets is very low. The mmWave vehicles can access RSUs over mmWave channels within a distance of r_{V2I} and communicate with each other only when they are within a distance of r_{V2V} and there are no vehicles blocking their LOS paths. The controllable vehicles can change their relative positions on the road in order to expand coverage, while uncontrollable vehicles do not change their relative positions or move randomly because they have other driving strategies or are driven by humans.

Let n , n_m , and n_c denote the total number of vehicles, all mmWave vehicles, and the number of controllable mmWave vehicles in the RoI, respectively. $R_{mm} := n_m/n$ and $R_c := n_c/n_m$ denote the ratio of the number of the mmWave vehicles to the total number of vehicles and the ratio of the number of the controllable vehicles to the total number of mmWave vehicles, respectively. Let P_a , P_n , P_c , and P_u denote the sets of all grid positions in the RoI, the non-mmWave vehicle positions, the controllable mmWave vehicle positions, and the uncontrollable mmWave vehicle positions, respectively. $P_c \in \mathcal{P}$ is a variable that the proposed method controls, where $\mathcal{P} := 2^{P_a \setminus (P_n \cup P_u)}$ represents a power set of $P_a \setminus (P_n \cup P_u)$.

We define a quality metric for the proposed method as the proportion of areas where vehicles can connect to RSUs through multi-hop relay chains based on the coverage of each vehicle. When using mmWave vehicles as relay nodes, the mmWave V2I communication range of vehicle i is expressed as $r_i = 2r_{V2I} + l_i(P_c)$, as shown in Fig. 2. Here, $l_i(P_c)$ denotes the length along the x axis of the relay chains to which vehicle i belongs. Because RSUs are deployed at intervals of d , it is sufficient to consider d -long sections of road. The coverage for vehicle i is expressed as follows:

$$C_i(P_c) = \min \left\{ \frac{r_i}{d}, 1 \right\}. \quad (1)$$

Note that the coverage $C_i(P_c)$ increases linearly with the length of the multi-hop relay chain. Now, we define the average of the vehicles' coverage as a quality metric, as follows:

$$C_{avg}(P_c) := \frac{1}{n_m} \sum_{i=1}^{n_m} C_i(P_c). \quad (2)$$

Figure 3 shows an example of expanding coverage by changing vehicle positions. Non-mmWave, controllable mmWave, and uncontrollable mmWave vehicles are depicted as red, dark blue, and light blue vehicles in Fig. 3, respectively. Vehicles #1–#5 are all mmWave vehicles, but only vehicles #1 and #5 are controllable. Before vehicles #1 and #5 move, the relay chains on the left and right sides cannot be connected using the mmWave bands because they are out of

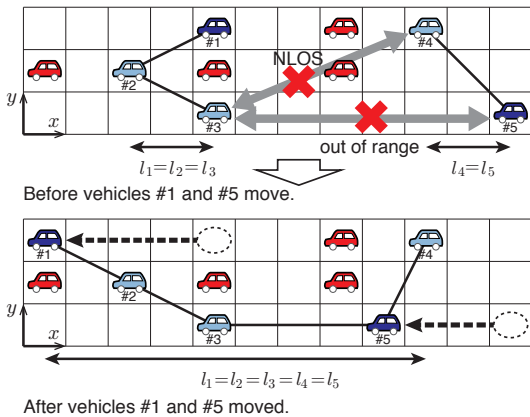


Fig. 3 Non-mmWave, controllable mmWave, and uncontrollable mmWave vehicles are depicted as red, dark blue, and light blue vehicles, respectively. The mmWave relay length is extended by changing the positions of vehicles #1 and #5.

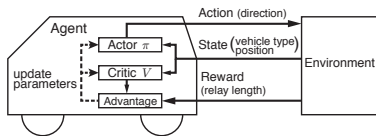


Fig. 4 Actor-critic reinforcement learning model

communication range or non-mmWave vehicles are blocking the LOS. However, after vehicles #1 and #5 move, vehicles #3 and #5 become connected. At this point, all mmWave vehicles can be connected, and the length of the relay chain is extended. $C_{\text{avg}}(P_c)$ increases as a result.

4. Distributed Vehicle Movement Controls

4.1 Motivation for Using Reinforcement Learning

Although we revealed the capability of coverage improvement using vehicle position control in [17], solving the vehicle-movement problem is still a big challenge. Because vehicle-moving strategies should be scalable and decentralized for practical usage, each vehicle should be able to decide its movement for increasing coverage by itself. Because of conventional microwave communication systems, information on the surrounding vehicles' positions are available for each controllable vehicle to decide its movement. We formulate the decision-making problem as an MDP such that it can be solved by RL. Using the RL scheme, vehicles can learn the optimal positions to increase coverage and go there without being instructed to. Because the observed states have large dimensions, traditional RL methods cannot be applied to our problem; thus, a DeepRL algorithm is required for

function approximation. We utilize the DeepRL algorithm, A3C, because it is advantageous in terms of convergence efficiency and learning speed [19].

While vehicles are learning strategies using the A3C algorithm, they share DNN models with other vehicles. To this end, we assume there is a model management server that stores a global model. The model management server updates the global model using gradients collected from the vehicles and distributes the up-to-date model to the vehicles. These data are transmitted via microwave channels or mmWave relays if they are available. In this system, vehicles do not always have to be connected to the model management server. They opportunistically upload their gradient, and then, the model management server updates the global model. Once the well-trained model is obtained, there is no need for vehicles to share DNN models during the operation phase. Therefore, controllable vehicles decide their movements by using the model in a decentralized way. In the following portion of this section, we explain how vehicles learn movement strategies of coverage expansion using the RL algorithm. We also describe state designs that improve the performance of increasing coverage.

4.2 Deep-Reinforcement-Learning-Based Algorithm

Controllable vehicles, called agents, interact with an environment over a number of discrete time steps. The relationship between an agent and the environment is shown in Fig. 4. At each time step t , agent i observes the surrounding states $s_{i,t}$ representing other vehicles' positions and types. The detailed definitions of the states are given by (7), (8), and (9) in Section 4.3. The surrounding vehicle information is shared via microwave channels, and the observation range is limited by the microwave communication range, which determines the dimension of the states. The observation area is limited by the range of DSRC communications, where positions and types of vehicles are broadcasted and shared with each other. According to an action-selection policy $\pi(a_{i,t}|s_{i,t})$, agents select an action $a_{i,t}$ from a set of actions \mathcal{A} consisting of *forward*, *back*, *right*, *left*, and *stay*. Note that these actions represent changing relative positions with respect to the other vehicles. After moving to the next position, agent i receives a reward $r_{i,t}$. A reward from each step is defined as:

$$r_{i,t} := \begin{cases} \alpha l_i + r_p & \text{if an agent selects a prohibited direction} \\ \alpha l_i & \text{otherwise,} \end{cases} \quad (3)$$

where l_i and $\alpha (> 0)$ denote a relay length and parameter balancing the reward and penalty, respectively. $r_p (< 0)$ denotes a penalty that is added when an agent selects a direction, where the vehicle should not move. In order to avoid car accidents, the prohibited direction is defined as the direction where other vehicles exist or are moving to and where the agent gets off the road. Relay length information is calculated by the following procedure. Agents broadcast their

position information via the relay over the mmWave channel. Then, the agents calculate the relay length l_i as the length along the road direction between the head and tail vehicles using shared position information. Such information sharing can be completed within a short period compared to the decision-making interval of the RL scheme.

The goal of RL is to optimize the action-selection policy $\pi(a_{i,t}|s_{i,t})$ to maximize the future accumulated reward $R_{i,t} := \sum_{\tau=0}^{\infty} \gamma^\tau r_{i,t+\tau}$, where $\gamma \in [0, 1)$ is a discount factor. The expectation of $R_{i,t}$ from step t underlying π is called the value function, which is defined as $V^\pi(s_{i,t}) := \mathbb{E}[R_{i,t}|s_{i,t}]$. Each agent acts to maximize its own accumulated reward $R_{i,t}$, which can be calculated from information obtained by the agent; thus, our system works in a distributed manner.

We employ A3C [19] as the implementation of DeepRL. A3C learns the optimal policy with sharing models and experiences by multiple agents; thus, it suits our problem in which multiple vehicles are required to learn a similar strategy. Algorithm 1 shows the detailed procedure of the A3C learning phase in each episode, which consists of T_{\max} time steps. For more detail, please refer to [19]. A3C parameterizes the policy function $\pi(a_{i,t}|s_{i,t}; \theta)$ and the value function $V(s_{i,t}; \theta_v)$, where θ and θ_v denote globally shared parameters of π and V , respectively. The globally shared parameters are stored in the model management server. Agents first download the globally shared parameters and copy them to agent-specific parameters θ_i and $\theta_{v,i}$ when they have started learning (Line 3 in Algo. 1). The agents act t_{\max} times in accordance with their agent-specific policies independently and store rewards from each step (Lines 4–9 in Algo. 1). The agents calculate the gradients of updating parameters $\Delta\theta_i$ and $\Delta\theta_{v,i}$ at interval t_{\max} (Lines 10–17 in Algo. 1). The calculated gradients are uploaded to the model management server, and then, the server updates the globally shared parameters θ and θ_v by gradient ascent and gradient descent, respectively (Lines 18–19 in Algo. 1). After sufficient time steps, the shared policy and value functions each converge to the corresponding optimal functions. The gradients $\Delta\theta_i$ and $\Delta\theta_{v,i}$ are calculated as follows:

$$\theta: \Delta\theta_i = \sum_{\tau=t}^{t+t_{\max}} \nabla_{\theta_i} \log \pi(a_{i,\tau}|s_{i,\tau}; \theta_i) A(a_{i,\tau}, s_{i,\tau}; \theta_{v,i}) + \beta \nabla_{\theta_i} H(\pi(s_{i,\tau}; \theta_i)), \quad (4)$$

$$\theta_v: \Delta\theta_{v,i} = c_v \sum_{\tau=t}^{t+t_{\max}} \partial (A(a_{i,\tau}, s_{i,\tau}; \theta_{v,i}))^2 / \partial \theta_{v,i}, \quad (5)$$

where β , $H(\pi(s_{i,\tau}; \theta_i))$, and c_v denote a regularization parameter, the entropy of $\pi(s_{i,\tau}; \theta_i)$, and a coefficient that balances θ and θ_v , respectively. $A(a_{i,\tau}, s_{i,\tau}; \theta_{v,i})$ is an estimation of the advantage of action $a_{i,\tau}$ in state $s_{i,\tau}$ [19], defined as:

$$A(a_{i,\tau}, s_{i,\tau}; \theta_{v,i}) := \sum_{u=0}^{\tau'-1} \gamma^u r_{i,\tau+u} + \gamma^{\tau'} V(s_{i,\tau+\tau'}; \theta_{v,i}) - V(s_{i,\tau}; \theta_{v,i}), \quad (6)$$

where τ' is a counter that is incremented at each step in the

Algorithm 1 Algorithm for updating policy and value model parameters.

```

1: Initialize  $t \leftarrow 0$ .
2: while  $t < T_{\max}$  do
3:   Download the globally shared parameters and copy them to agent-
     specific parameters:  $\theta_i \leftarrow \theta$ ,  $\theta_{v,i} \leftarrow \theta_v$ .
4:    $t_{\text{start}} \leftarrow t$ 
5:   for  $t \in \{t_{\text{start}}, \dots, t_{\text{start}} + t_{\text{max}}\}$  do
6:     perform action  $a_{i,t}$  according to policy  $\pi(a_{i,t}|s_{i,t}; \theta_i)$ 
7:     receive reward  $r_{i,t}$ 
8:      $t \leftarrow t + 1$ 
9:   end for
10:  Reset gradients  $\Delta\theta_i$  and  $\Delta\theta_{v,i}$  to 0.
11:   $R_{i,t} \leftarrow V(s_{i,t}; \theta_{v,i})$ 
12:  for  $\tau \in \{t_{\text{start}} + t_{\text{max}} - 1, \dots, t_{\text{start}}\}$  do
13:     $R_{i,\tau} \leftarrow r_{i,\tau} + \gamma R_{i,\tau+1}$ 
14:     $A(a_{i,\tau}, s_{i,\tau}; \theta_{v,i}) \leftarrow R_{i,\tau} - V(s_{i,\tau}; \theta_{v,i})$ 
15:     $\Delta\theta_i \leftarrow \Delta\theta_i + \nabla_{\theta_i} \log \pi(a_{i,\tau}|s_{i,\tau}; \theta_i) A(a_{i,\tau}, s_{i,\tau}; \theta_{v,i}) +$ 
       $\beta \nabla_{\theta_i} H(\pi(s_{i,\tau}; \theta_i))$ 
16:     $\Delta\theta_{v,i} \leftarrow \Delta\theta_{v,i} + c_v \partial (A(a_{i,\tau}, s_{i,\tau}; \theta_{v,i}))^2 / \partial \theta_{v,i}$ 
17:  end for
18:  Upload gradients  $\Delta\theta_i$  and  $\Delta\theta_{v,i}$  to the server
19:  [SERVER] Update parameters  $\theta$  and  $\theta_v$ 
20: end while

```

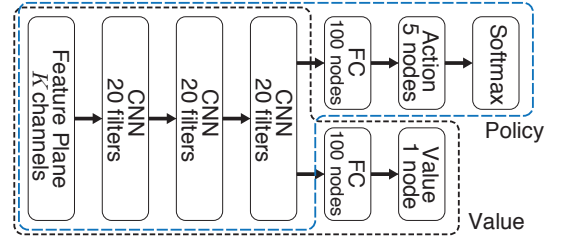


Fig. 5 DNN models of policy and value functions.

loop (Line 12–17 in Algo. 1).

In a common A3C learning phase, multiple agents in multiple independent environments share the parameters θ and θ_v of the learning models. This model sharing enables efficient convergence due to the independence between training data sets. Although there is a single environment in our problem, the observed states of multiple agents are different and have little correlation if their distances are great enough. DNN models therefore converge due to model sharing.

4.3 State Designs and Network Models

We designed three state definitions: (1) vehicle positions and types (PT); (2) vehicle positions, types, and continuous relay lengths (PTCL); and (3) vehicle positions, types, and discrete relay lengths (PTDL). We compared the performance of these state definitions in Section 5 and showed that PTCL and PTDL, which include relay length information, achieve greater coverage than PT.

States $s_{i,t}$ are defined as three-dimensional $K \times X \times Y$ feature planes, where K , X , and Y denote the number of features and the observation ranges of the x and y axes,

respectively. A feature plane design is introduced in AlphaGo [32]. Feature planes represent different features in different planes and convolutional neural networks (CNN) are expected to adaptively optimize their parameters to each feature. Let $s_{i,t}^{(k,x,y)}$ denote each state element, where k and (x, y) represent a feature index and a relative position observed from the vehicle i , respectively. The center of each feature plane represents the position of vehicle i . While X is limited by the microwave communication range, Y is defined as $Y := 2N_1 - 1$ to cover all lanes. The state elements $s_{i,t}^{(k,x,y)}$ in PT are defined as follows:

$$s_{i,t}^{(1,x,y)} := \begin{cases} 1 & \text{if a mmWave vehicle positions at } (x, y), \\ 0 & \text{otherwise,} \end{cases} \quad (7)$$

$$s_{i,t}^{(2,x,y)} := \begin{cases} 1 & \text{if a non-mmWave vehicle positions at } (x, y), \\ 0 & \text{otherwise,} \end{cases} \quad (8)$$

$$s_{i,t}^{(3,x,y)} := \begin{cases} 1 & \text{if } (x, y) \text{ is empty,} \\ 0 & \text{otherwise.} \end{cases} \quad (9)$$

In order to improve the coverage performance of RL-based methods, we designed states with additional information regarding the achievable relay length $\hat{l}_i(x, y)$ when vehicle i would move to position (x, y) . $\hat{l}_i(x, y)$ is calculated by each agent using vehicle positions and type information. Each agent is required to estimate whether a stable mmWave communication link could be established to calculate $\hat{l}_i(x, y)$. Link stability can be estimated using path-loss prediction models [6, 35], which enable vehicles to predict path loss considering blockage effects caused by other vehicles. Margins can be considered for the received power required to establish links in order to avoid misprediction. Additional PTCL features are defined as follows:

$$s_{i,t}^{(4,x,y)} := \rho \hat{l}_i(x, y), \quad (10)$$

where ρ denotes a normalization factor. The features for $k = 1, 2, 3$ are defined to be the same as PT.

In contrast to PTCL, relay length $\hat{l}_i(x, y)$ of PTDL is encoded to one-hot vectors, which are employed in AlphaGo [32]. State elements for $k \in \{4, \dots, K\}$ are defined as follows:

$$s_{i,t}^{(k,x,y)} := \begin{cases} 1 & \text{if } \hat{l}_i(x, y) \in \mathcal{R}_k, \\ 0 & \text{otherwise,} \end{cases} \quad (11)$$

$$\begin{aligned} \mathcal{R}_4 &:= \{0\}, \\ \mathcal{R}_k &:= (L_k, L_{k+1}] \quad \text{for } k = 5, \dots, K-1, \\ \mathcal{R}_K &:= (L_K, \infty), \end{aligned} \quad (12)$$

where L_k denotes a border series used to encode relay lengths $\hat{l}_i(x, y)$ into one-hot vectors.

After pre-processing, states $s_{i,t}$ are input into a policy function π and a value function V . Their DNN models are shown in Fig. 5. The lower CNN layers are shared by two

Table 1 Simulation parameters.

Parameters	Values
Length of RoI	1 km
Number of lane N_1	4
Number of grids	200×4
Lane width	3.5 m
RSU interval d	1 km
mmWave V2V communication range r_{V2V}	50 m
mmWave V2I communication range r_{V2I}	100 m
Size of the observation area $X \times Y$	41×7
Normalization factor for PTCL ρ	0.005 m^{-1}
The number of features of PTDL K	9
Boarder series of PTDL L_k ($k = 5, \dots, 9$)	0, 25, 50, 100, 150
Reward balancing parameter α	0.5 m^{-1}
Penalty r_p	-2
Discount factor γ	0.1
Maximum time steps per episode T_{\max}	100
Number of episodes (learning phase)	300
Number of episodes (test phase)	100
Update intervals t_{\max}	2
Regularization parameter β	0.01
Optimizer	Shared RMSProp [19]
Coefficient of balancing gradients c_v	0.5

functions, and the higher fully connected (FC) layers are separated. Such a shared model is used in [19].

5. Simulation Evaluations

5.1 Simulation Setup

In the simulations, the vehicles were located at randomly selected grid points. Let λ denote the density of vehicles in each lane. Vehicle types were determined randomly according to the ratio R_{mm} and R_c . The controllable vehicles had their actions controlled by the proposed RL algorithm. On the other hand, the non-mmWave vehicles and uncontrollable vehicles did not change their relative positions or selected action among *forward*, *stay*, and *back* in order to simulate two scenarios where they drive at equal and constant velocities and where they change their velocities randomly. If more than one vehicle selected the same grid, the vehicle that had the highest priority moved to the selected grid, while the others did not change their positions. Penalties were given to vehicles that could not move to the selected grid. The priority was defined as follows:

- Non-mmWave vehicles and uncontrollable vehicles have greater priority than controllable vehicles.
- Forward vehicles have greater priority if their types are the same.
- Vehicles with small y position values have greater priority if their types and x position values are the same.

The first rule is applied to prevent the proposed method from interrupting the other vehicles' movement. The second one simulates the realistic driving manners. To simplify the simulation, we also apply the third one. The mmWave vehicles could communicate with each other over the mmWave band if the distance between them was less than 50 m. Blocking

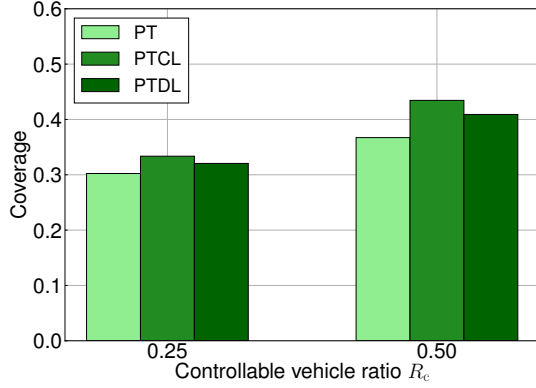


Fig. 6 Coverage of different state designs when $\lambda = 0.02$ veh/m/lane and $R_{\text{mm}} = 0.4$. Uncontrollable vehicles move at constant velocities. The results of PTCL and PTDL are greater coverage than that of PT.

by other vehicles is detected as follows: We draw a line from the sender to the receiver and list the grid sections that cross the line. If there is no vehicle on the listed grid sections, the sender and the receiver can communicate with each other via LOS path. We also assumed that link qualities of the mmWave channels are ideally predictable in our simulations.

We performed python-based simulations to determine the performance of the movement strategy based on DeepRL. The RL simulations consist of two phases, the learning and test phases. In the learning phase, the controllable vehicles move around and update their RL models according to Algorithm 1. We perform 300 episodes in our simulations. At the beginning of each episode, non-mmWave vehicles and uncontrollable vehicles are relocated randomly in order to obtain a general strategy. We obtain some models which are learned under different conditions: the vehicle density, ratio of mmWave vehicles, and ratio of controllable vehicles. We assume the conditions are stable while learning each model. In the test phase, we evaluate the performance of the globally shared policy models obtained from the learning phases. At the beginning of the evaluations, the shared policy models are copied to agent-specific models and they are not updated while being evaluated. The conditions in the learning and testing phases can be different, and we compare the performance of the different models for the same evaluation conditions. The RL simulation parameters and their values are listed in Table 1.

5.2 Performance of Reinforcement-Learning-Based Method

The coverage performance with three types of states PT, PTCL, and PTDL when $\lambda = 0.02$ veh/m/lane and $R_{\text{mm}} = 0.4$ is shown in Fig. 6. It can be seen that PTCL and PTDL achieve higher performance than PT, which means that additional relay length information improves the performance of RL-based methods.

Figures 7 and 8 show the coverage performance and

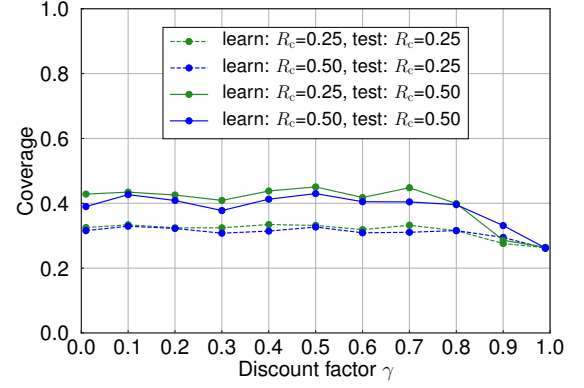


Fig. 7 Coverage for different discount factors γ when $\lambda = 0.02$ veh/m/lane, $R_{\text{mm}} = 0.4$, and PTCL is used as the state type. Uncontrollable vehicles move at constant velocities. Policies learned when $\gamma \leq 0.8$ show higher performance.

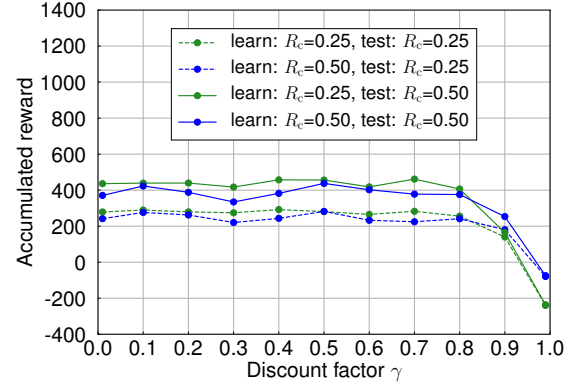


Fig. 8 Accumulated reward for different discount factors γ when $\lambda = 0.02$ veh/m/lane, $R_{\text{mm}} = 0.4$, and PTCL is used as the state type. Uncontrollable vehicles move at constant velocities.

accumulated reward with different discount factors when $\lambda = 0.02$ veh/m/lane, $R_{\text{mm}} = 0.4$, and the state type is PTCL. When the discount factor γ is greater than 0.8, the coverage decreases. In particular, when $\gamma = 0.99$, the accumulated rewards are less than zero, which means that agents failed to learn a reasonable policy under the hyper parameter settings and the simulation scenarios.

The coverage and accumulated reward as functions of time step t are shown in Fig. 9. Simulations are performed under two conditions where non-mmWave vehicles and uncontrollable vehicles run at equal and constant velocities and where they change their velocities randomly. In both conditions, the coverage increases as the agents change their positions. Coverage is greater when uncontrollable vehicles move at the same velocity, than when uncontrollable vehicles move at different velocities. Accumulated reward increases linearly even when $t > 75$ because nearly constant rewards are given to agents after the coverage converges.

Coverage and accumulated reward as functions of the

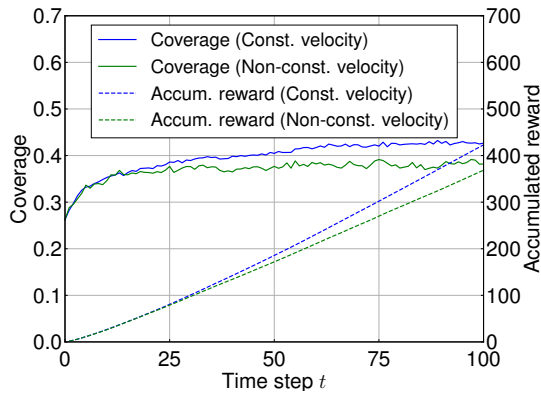


Fig. 9 Coverage and accumulated reward as functions of time steps when $\lambda = 0.02$ veh/m/lane, $R_{\text{mm}} = 0.4$, $R_c = 0.5$, and PTCL is used as the state type. Accumulated rewards increase linearly even after coverage becomes constant.

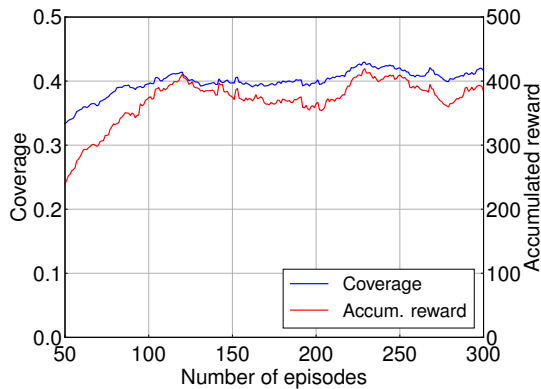


Fig. 10 Moving average of coverage and accumulated reward as functions of the number of training episodes when $\lambda = 0.02$ veh/m/lane, $R_{\text{mm}} = 0.4$, $R_c = 0.5$, and PTCL is used as the state type. Uncontrollable vehicles move at constant velocities.

number of episodes in learning phases are shown in Fig. 10. 50-episode moving averages are shown because the achievable coverage in each episode varies due to the random variables such as the number of vehicles and initial vehicle positions. It is shown that coverage and accumulated reward increase at first, and then do not increase when the number of episodes is greater than 120. This is because various experiences improve agents' strategies at first, whereas additional experiences do not contribute to improving the strategies as much after the agents have learned from many experiences.

In Fig. 11, the coverage performance with different models obtained in different learning conditions is shown. We trained 20 models in learning environments with varying R_c and R_{mm} , transferred them to test environments with $R_{\text{mm}} = 0.4, 0.7, 1.0$, and evaluated coverage of the position controls using the models. The models learned when $0.3 \leq R_{\text{mm}} \leq 0.7$ show approximately the same performance, which means these models can be applied when the

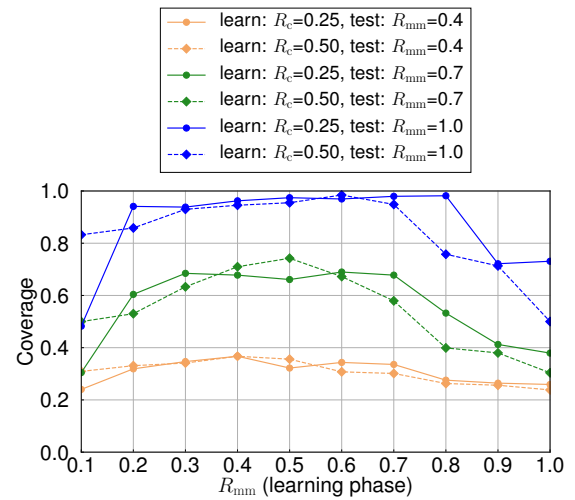


Fig. 11 Coverage of models learned in different learning conditions R_{mm} and R_c when $\lambda = 0.02$ veh/m/lane. PT is used as the state type and uncontrollable vehicles move at constant velocities. The models learned when $0.3 \leq R_{\text{mm}} \leq 0.7$ show relatively higher performance.

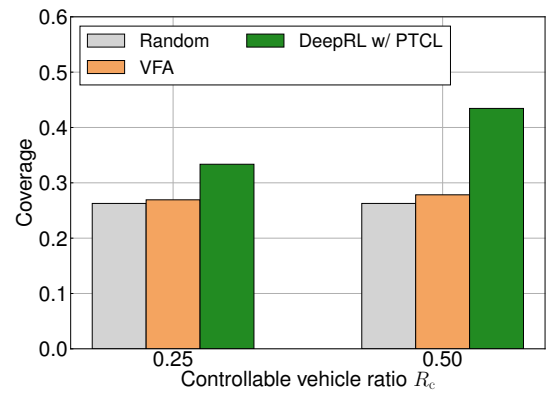


Fig. 12 Coverage of different movable methods when $\lambda = 0.02$ veh/m/lane, $R_{\text{mm}} = 0.4$ and uncontrollable vehicles move at constant velocities. RL shows higher performance than random and VFA.

penetration ratio is changed from that in the learning phases. On the other hand, the models learned when $R_{\text{mm}} \geq 0.9$ show lower performance. When there are many mmWave vehicles in the learning phases, large coverage can be achieved without movement of agents. Therefore, the agents cannot learn aggressive moving policies. This is why the models learned with large R_{mm} show lower performance. The models learned when $R_c = 0.25$ and $R_{\text{mm}} = 0.1$ also show lower performance. This is because the number of agents is too small to learn policies that increase coverage.

The coverage performance of the RL-based method with PTCL is compared with that of random positions and VFA under conditions when $\lambda = 0.02$ veh/m/lane, $R_{\text{mm}} = 0.4$, and uncontrollable vehicles move at constant and equal velocities in Fig. 12. As a comparative method, we use

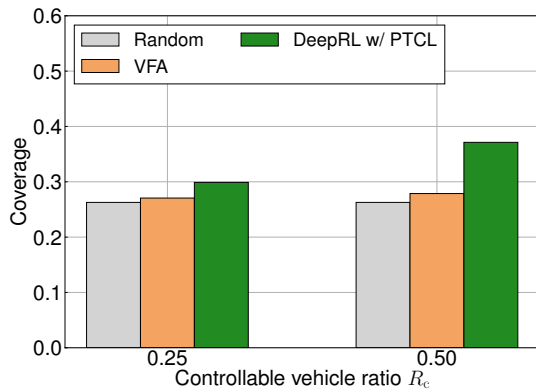


Fig. 13 Coverage of different movable methods when $\lambda = 0.02$ veh/m/lane, $R_{mm} = 0.4$ and uncontrollable vehicles move at random velocities. RL shows higher performance than random and VFA.

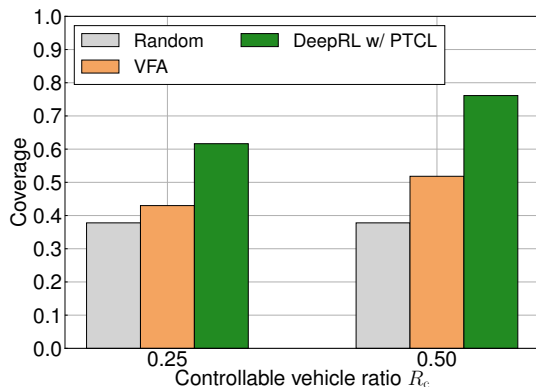


Fig. 14 Coverage of different movable methods when $\lambda = 0.01$ veh/m/lane, $R_{mm} = 1$ and uncontrollable vehicles move at constant velocities.

exponential VFA [25] with parameters $W_a = 1$, $W_r = 10000$, $\beta_1 = \beta_2 = 2$, and $D_{th} = 50$ m. Details of these parameters are described in [25]. The coverage achieved with the RL-based method is higher than the coverage of random positions and VFAs. For example, the coverage obtained from the RL-based method is about 1.7 times the coverage obtained with random positions when $R_c = 0.5$. Although vehicles with VFA adjust distances between themselves in order to connect with each other, they do not consider blockage of mmWave communications. On the other hand, vehicles with RL agents optimize their actions to expand their coverage following the learned policy models. Consequently, the performance of DeepRL exceeds that of VFA.

The coverage performance with different method is compared with that of random positions and VFA under conditions when $\lambda = 0.02$ veh/m/lane, $R_{mm} = 0.4$, and uncontrollable vehicles move at different velocities in Fig. 13. It is notable that the performance of the proposed method exceeds that of VFA even when the vehicles move at different velocities.

Coverage performance when $\lambda = 0.01$ veh/m/lane, $R_{mm} = 1$, and uncontrollable vehicles move at constant and equal velocities is shown in Fig. 14. The training of the RL-based methods were conducted under the conditions with $\lambda = 0.02$ and $R_{mm} = 0.4$, and the model transferred to this evaluation environment. The RL performance shows larger coverages than the results with $R_{mm} = 0.4$ in Fig. 12 because there are fewer obstacles that disrupt the movement of the controllable vehicles (i.e., RL agents) and thus, they easily move to positions where long relays can be achieved. Furthermore, VFAs show lower performance than the RL-based methods because they rely on the assumption that all vehicles are controllable while they are not in the environment.

5.3 Comparisons with Other RL Algorithm

Here, we discuss other RL algorithms compared with one used in the proposed method for the position control problem. As introduced in [30], there are many RL algorithms. The table-based Q-learning is one of most widely used algorithm for various problems. However, the algorithm is not suitable for our problem because it requires large memory capacity, whereas it is difficult for vehicles to have large memory. In the table-based Q-learning, an action-value function is represented as a table, called Q table, and the memory capacity required to store the table is proportional to the number of values that the state $s_{i,t}$ can take. In our problem, it increases exponentially with the observation range $X \times Y$; thus, the table-based Q-learning is difficult to apply for our problem when the observation range becomes large.

DQN [31] can be a candidate algorithm for our problem. DQN utilizes DNN to approximate an action-value function instead of using the Q table; thus, the required memory capacity can be small when the state is large. However, DQN cannot leverage experiences obtained by multiple vehicles while the vehicles try to learn similar strategies, because the algorithm is designed for single-agent problems.

There are several multi-process DeepRL algorithms, which can be applied to multi-agent environments. The DeepRL algorithms can leverage experiences of multiple agent to update a model; thus, it can learn a strategy faster and the strategy can be achieved higher performance than single-agent RL algorithm [19, 33]. We applied A3C [19] to our problems in this paper as a state-of-the-art multi-process DeepRL algorithm, and we showed that the proposed method increases coverage in our problem. Since the focus of our paper is not on designing or determining the best RL algorithm for the problem, the detailed performance comparison between A3C and other multi-agent RL algorithms is out of our scope.

6. Conclusions and Future Works

We proposed a vehicle position control method for mmWave vehicular networks that increases coverage through multi-hop V2V relaying. We adopted A3C, which is one of the state-of-the-art of RL methods, to obtain practical move-

ment strategies and designed states with relay length information that improved system performance in terms of increasing coverage. We also showed that the RL-based strategy achieved 1.7 times the coverage of random positions when the penetration ratio of mmWave vehicles was 40% and half of the mmWave vehicles employed the proposed RL algorithm. Moreover, the RL-based strategy increased coverage, even when the vehicle density and penetration ratio of mmWave vehicles differed from those of the learning phase.

Our future work includes evaluating the performance of the proposed method with metrics other than relay length. One of the advantages of RL is applicability for tasks with other objectives by redesigning the reward. For example, the reliability and connectivity of the multi-hop network is more important than relay length when the vehicular network is used for safety applications or vehicular cloud computing. The proposed method has potential to achieve such objectives; thus, we will demonstrate the performance in our future work.

A method to share and aggregate models learned by the vehicles to improve their performance is also included in our future work. Current work assumed that the model sharing is conducted ideally, i.e., the sharing is done without delay, loss, and bandwidth consumption. The model-sharing method should be designed in consideration of scalability, delay, loss, and bandwidth consumption of wireless communications.

Acknowledgment

This work was supported in part by JSPS KAKENHI Grant Number 17H03266, KDDI Foundation, and Tateisi Science and Technology Foundation.

References

- [1] N. Lu, N. Cheng, N. Zhang, X. Shen, and J.W. Mark, "Connected vehicles: Solutions and challenges," *IEEE Internet of Things Journal*, vol.1, no.4, pp.289–299, May 2014.
- [2] M. Gerla, E.K. Lee, G. Pau, and U. Lee, "Internet of vehicles: From intelligent grid to autonomous cars and vehicular clouds," *Proc. of IEEE World Forum on Internet of Things (WF-IoT)*, pp.241–246, March 2014.
- [3] V. Va, T. Shimizu, G. Bansal, and R.W. Heath Jr., "Millimeter wave vehicular communications: A survey," *Foundations and Trends in Networking*, vol.10, no.1, pp.1–113, June 2016.
- [4] M. Gerla, "Vehicular cloud computing," 2012 The 11th Annual Mediterranean Ad Hoc Networking Workshop (Med-Hoc-Net), pp.152–155, June 2012.
- [5] V. Semkin, U. Virk, A. Karttunen, K. Haneda, and A.V. Räsänen, "E-band propagation channel measurements in an urban street canyon," 9th European Conference on Antennas and Propagation (EuCAP), pp.1–4, IEEE, April 2015.
- [6] A. Yamamoto, K. Ogawa, T. Horimatsu, A. Kato, and M. Fujise, "Path-loss prediction models for intervehicle communication at 60 GHz," *IEEE Transactions on Vehicular Technology*, vol.57, no.1, pp.65–78, Jan. 2008.
- [7] C. Wu, T. Yoshinaga, and Y. Ji, "Cooperative content delivery in vehicular networks with integration of sub-6 GHz and mmWave," *Globecom Workshops*, 2017 IEEE, pp.1–6, IEEE, Dec. 2017.
- [8] H. Zhou, B. Liu, T.H. Luan, F. Hou, L. Gui, Y. Li, Q. Yu, and X. Shen, "Chaincluster: Engineering a cooperative content distribution framework for highway vehicular communications," *IEEE Transactions on Intelligent Transportation Systems*, vol.15, no.6, pp.2644–2657, Dec. 2014.
- [9] A. Benslimane, T. Taleb, and R. Sivaraj, "Dynamic clustering-based adaptive mobile gateway management in integrated VANET – 3G heterogeneous wireless networks," *IEEE Journal on Selected Areas in Communications*, vol.29, no.3, pp.559–570, March 2011.
- [10] P. Salvo, F. Cuomo, A. Baiocchi, and A. Bragagnini, "Road side unit coverage extension for data dissemination in VANETs," *Wireless On-demand Network Systems and Services (WONS)*, 2012 9th Annual Conference on, pp.47–50, IEEE, Jan. 2012.
- [11] M. Amoozadeh, H. Deng, C.N. Chuah, H.M. Zhang, and D. Ghosal, "Platoon management with cooperative adaptive cruise control enabled by VANET," *Vehicular communications*, vol.2, no.2, pp.110–123, April 2015.
- [12] P. Fernandes and U. Nunes, "Platooning with IVC-enabled autonomous vehicles: Strategies to mitigate communication delays, improve safety and traffic flow," *IEEE Transactions on Intelligent Transportation Systems*, vol.13, no.1, pp.91–106, March 2012.
- [13] J.A. Fax and R.M. Murray, "Information flow and cooperative control of vehicle formations," *IEEE Transactions on Automatic Control*, vol.49, no.9, pp.1465–1476, Sept. 2004.
- [14] R. Olfati-Saber and R.M. Murray, "Distributed cooperative control of multiple vehicle formations using structural potential functions," *IFAC Proceedings Volumes*, vol.35, no.1, pp.495–500, July 2002.
- [15] P. Basu and J. Redi, "Movement control algorithms for realization of fault-tolerant ad hoc robot networks," *IEEE Network*, vol.18, no.4, pp.36–44, July 2004.
- [16] S. Gundry, J. Zou, C.S. Sahin, J. Kusyk, and M.U. Uyar, "Autonomous and fault tolerant vehicular self deployment mechanisms in MANETs," *Technologies for Homeland Security (HST)*, 2013 IEEE International Conference on, pp.595–600, IEEE, Nov. 2013.
- [17] A. Taya, T. Nishio, M. Morikura, and K. Yamamoto, "Coverage expansion through dynamic relay vehicle deployment in mmwave V2I communications," 2018 IEEE 87th Vehicular Technology Conference (VTC Spring), pp.1–5, IEEE, June 2018.
- [18] P. Raja and S. Pugazhenthii, "Optimal path planning of mobile robots: A review," *International Journal of Physical Sciences*, vol.7, no.9, pp.1314–1320, Feb. 2012.
- [19] V. Mnih, A.P. Badia, M. Mirza, A. Graves, T. Lillicrap, T. Harley, D. Silver, and K. Kavukcuoglu, "Asynchronous methods for deep reinforcement learning," *The 33rd International Conference on Machine Learning*, pp.1928–1937, June 2016.
- [20] D. Jiang, V. Taliwal, A. Meier, W. Holfelder, and R. Herrtwich, "Design of 5.9 GHz DSRC-based vehicular safety communication," *IEEE Wireless Communications*, vol.13, no.5, Oct. 2006.
- [21] R. Molina-Masegosa and J. Gozalvez, "LTE-V for sidelink 5G V2X vehicular communications: A new 5G technology for short-range vehicle-to-everything communications," *IEEE Vehicular Technology Magazine*, vol.12, no.4, pp.30–39, Dec. 2017.
- [22] R. Verdone, "Multihop R-ALOHA for intervehicle communications at millimeter waves," *IEEE Transactions on Vehicular Technology*, vol.46, no.4, pp.992–1005, Nov. 1997.
- [23] T. Paul, T.R. Krogstad, and J.T. Gravdahl, "Modelling of UAV formation flight using 3D potential field," *Simulation Modelling Practice and Theory*, vol.16, no.9, pp.1453–1462, Oct. 2008.
- [24] X. Yu, W. Huang, J. Lan, and X. Qian, "A novel virtual force approach for node deployment in wireless sensor network," *Proc. of IEEE 8th International Conference on Distributed Computing in Sensor Systems*, pp.359–363, May 2012.
- [25] J. Chen, S. Li, and Y. Sun, "Novel deployment schemes for mobile sensor networks," *Sensors*, vol.7, no.11, pp.2907–2919, Nov. 2007.
- [26] W. Roh, J.Y. Seol, J. Park, B. Lee, J. Lee, Y. Kim, J. Cho, K. Cheun, and F. Aryanfar, "Millimeter-wave beamforming as an enabling technology for 5G cellular communications: theoretical feasibility and prototype results," *IEEE Communications Magazine*, vol.52, no.2,

pp.106–113, Feb. 2014.

- [27] E.M. Mohamed, K. Sakaguchi, and S. Sampei, “Millimeter wave beamforming based on WiFi fingerprinting in indoor environment,” IEEE International Conference on Communication Workshop (ICCW), pp.1155–1160, IEEE, June 2015.
- [28] N. González-Prelcic, R. Méndez-Rial, and R.W. Heath, “Radar aided beam alignment in mmWave V2I communications supporting antenna diversity,” Information Theory and Applications Workshop (ITA), pp.1–7, IEEE, Feb. 2016.
- [29] R.S. Sutton and A.G. Barto, Reinforcement learning: An introduction, MIT press Cambridge, 1998.
- [30] N.D. Nguyen, T. Nguyen, and S. Nahavandi, “System design perspective for human-level agents using deep reinforcement learning: A survey,” IEEE Access, vol.5, pp.27091–27102, Nov. 2017.
- [31] V. Mnih, K. Kavukcuoglu, D. Silver, A.A. Rusu, J. Veness, M.G. Bellemare, A. Graves, M. Riedmiller, A.K. Fidjeland, G. Ostrovski, *et al.*, “Human-level control through deep reinforcement learning,” Nature, vol.518, no.7540, pp.529–533, Feb. 2015.
- [32] D. Silver, A. Huang, C.J. Maddison, A. Guez, L. Sifre, G. Van Den Driessche, J. Schrittwieser, I. Antonoglou, V. Panneershelvam, M. Lanctot, *et al.*, “Mastering the game of go with deep neural networks and tree search,” Nature, vol.529, no.7587, pp.484–489, Jan. 2016.
- [33] A. Nair, P. Srinivasan, S. Blackwell, C. Alcicek, R. Fearon, A.D. Maria, V. Panneershelvam, M. Suleyman, C. Beattie, S. Petersen, S. Legg, V. Mnih, K. Kavukcuoglu, and D. Silver, “Massively parallel methods for deep reinforcement learning,” International Conference on Machine Learning (ICML) Deep Learning Workshop, July 2015.
- [34] R. Jiang and Q.S. Wu, “The adaptive cruise control vehicles in the cellular automata model,” Physics Letters A, vol.359, no.2, pp.99–102, Nov. 2006.
- [35] Y. Wang, K. Venugopal, A.F. Molisch, and R.W. Heath, “Analysis of urban millimeter wave microcellular networks,” Proc. of IEEE 84th Vehicular Technology Conference (VTC-Fall), pp.1–5, Sept. 2016.
- [36] H. Okamoto, T. Nishio, M. Morikura, K. Yamamoto, D. Murayama, and K. Nakahira, “Machine-learning-based throughput estimation using images for mmWave communications,” Proc. of IEEE 85th Vehicular Technology Conference (VTC Spring), pp.1–5, June 2017.
- [37] H. Okamoto, T. Nishio, M. Morikura, and K. Yamamoto, “Recurrent neural network-based received signal strength estimation using depth images for mmWave communications,” Proc. of IEEE Consumer Communications and Networking conference (CCNC) 2018, pp.1–2, Jan. 2018.



Akihito Taya received the B.E. degree in Electrical and Electronic Engineering from Kyoto University in 2011. He received the master degree in Communications and Computer Engineering, Graduate School of Informatics from Kyoto University, Kyoto, Japan, in 2013. He joined Hitachi, Ltd. in 2013, where he participated in the development of computer clusters. He is currently working toward a Ph.D. degree at the Graduate School of Informatics, Kyoto University. His current research interests include

vehicular communications and applications of machine learning. He is a student member of the IEEE, ACM, and IEICE.



Takayuki Nishio received the B.E. degree in Electrical and Electronic Engineering from Kyoto University in 2010. He received the master and Ph.D. degrees in Communications and Computer Engineering, Graduate School of Informatics from Kyoto University, Kyoto, Japan, in 2012 and 2013, respectively. From 2012 to 2013, he was a research fellow (DC1) of the Japan Society for the Promotion of Science (JSPS). Since 2013, He is an Assistant Professor in Communications and Computer Engineering, Graduate

School of Informatics, Kyoto University. From 2016 to 2017, he was a visiting researcher in Wireless Information Network Laboratory (WINLAB), Rutgers University, United States. His current research interests include mmWave networks, wireless local area networks, application of machine learning, and sensor fusion in wireless communications. He received IEEE Kansai Section Student Award in 2011, the Young Researcher’s Award from the IEICE of Japan in 2016, and Funai Information Technology Award for Young Researchers in 2016. He is a member of the IEEE, ACM, IEICE.



Masahiro Morikura Masahiro Morikura received his B.E., M.E., and Ph.D. degrees in electronics engineering from Kyoto University, Kyoto, Japan in 1979, 1981 and 1991, respectively. He joined NTT in 1981, where he was engaged in the research and development of TDMA equipment for satellite communications. From 1988 to 1989, he was with the Communications Research Centre, Canada, as a guest scientist. From 1997 to 2002, he was active in the standardization of the IEEE 802.11a based wireless

LAN. His current research interests include WLANs and M2M wireless systems. He received the Paper Award and the Achievement Award from IEICE in 2000 and 2006, respectively. He also received the Education, Culture, Sports, Science and Technology Minister Award in 2007 and Maejima Award in 2008, and the Medal of Honor with Purple Ribbon from Japan’s Cabinet Office in 2015. Dr. Morikura is now a professor in the Graduate School of Informatics, Kyoto University. He is a member of the IEEE.



Koji Yamamoto received the B.E. degree in electrical and electronic engineering from Kyoto University in 2002, and the M.E. and Ph.D. degrees in Informatics from Kyoto University in 2004 and 2005, respectively. From 2004 to 2005, he was a research fellow of the Japan Society for the Promotion of Science (JSPS). Since 2005, he has been with the Graduate School of Informatics, Kyoto University, where he is currently an associate professor. From 2008 to 2009, he was a visiting researcher at Wireless@KTH, Royal

Institute of Technology (KTH) in Sweden. He serves as an editor of IEEE Wireless Communications Letters from 2017 and the Track Co-Chairs of APCC 2017 and CCNC 2018. His research interests include radio resource management and applications of game theory. He received the PIMRC 2004 Best Student Paper Award in 2004, the Ericsson Young Scientist Award in 2006. He also received the Young Researcher’s Award, the Paper Award, SUEMATSU-Yasuharu Award from the IEICE of Japan in 2008, 2011, and 2016, respectively, and IEEE Kansai Section GOLD Award in 2012. He is a member of the IEEE.